



LAWRENCE  
LIVERMORE  
NATIONAL  
LABORATORY

# COG Validation for Foil and TLD Irradiation in a SILENE Criticality Excursion Benchmark Experiment

S. S. Kim, D. P. Heinrichs, R. M. Buck, E. M. Lent,  
C. K. Lee

January 4, 2016

PHYSOR 2016  
Sun Valley, ID, United States  
May 1, 2016 through May 5, 2016

## **Disclaimer**

---

This document was prepared as an account of work sponsored by an agency of the United States government. Neither the United States government nor Lawrence Livermore National Security, LLC, nor any of their employees makes any warranty, expressed or implied, or assumes any legal liability or responsibility for the accuracy, completeness, or usefulness of any information, apparatus, product, or process disclosed, or represents that its use would not infringe privately owned rights. Reference herein to any specific commercial product, process, or service by trade name, trademark, manufacturer, or otherwise does not necessarily constitute or imply its endorsement, recommendation, or favoring by the United States government or Lawrence Livermore National Security, LLC. The views and opinions of authors expressed herein do not necessarily state or reflect those of the United States government or Lawrence Livermore National Security, LLC, and shall not be used for advertising or product endorsement purposes.

# COG VALIDATION FOR FOIL AND TLD IRRADIATION IN A SILENE CRITICALITY EXCURSION BENCHMARK EXPERIMENT

Soon S. Kim, David P. Heinrichs, Richard M. Buck, Edward M. Lent, and Chuck K. Lee

Nuclear Criticality Safety Division

Lawrence Livermore National Laboratory, Livermore, California, USA

[kim53@llnl.gov](mailto:kim53@llnl.gov), [heinrichs1@llnl.gov](mailto:heinrichs1@llnl.gov), [buck2@llnl.gov](mailto:buck2@llnl.gov),  
[lent1@llnl.gov](mailto:lent1@llnl.gov), [lee12@llnl.gov](mailto:lee12@llnl.gov)

## ABSTRACT

COG is a Monte Carlo particle transport code developed by Lawrence Livermore National Laboratory (LLNL), and has been used mainly in nuclear criticality and radiation shielding applications for the past four decades. Three neutron excursion experiments performed at the CEA Valduc SILENE reactor in 2010 provided invaluable measurement data of foil and thermoluminescent dosimeters (TLDs) activation, allowing for testing of various COG functionalities including neutron activation, volume detector, and newly added delayed fission gamma ray options. Using COG, the SILENE reactor, experimental configurations, and surroundings were explicitly modeled in three dimensions for the first pulse experiment. In the model, the one-step CRITICALITY/DETECTOR option was activated for direct particle tracking from the reactor core to the detectors. In general, COG results agreed well with the measurement data except for concrete shielded foils and two cases where measurement data are believed to be in error. With the delayed fission gamma ray option activated, COG results compared well with the TLD dose measurement data. Because of direct particle tracking, significantly large computing time is required for good statistics. A new feature, Criticality Detector Variance Reduction (CritDetVR), is being incorporated into the source code to improve COG performance on a multiprocessor machine. With the new feature, variance reduction methods can be activated in a hybrid criticality/shielding calculation mode, which will result in significant computation time reduction. The latest version, COG11.1, which contains all these features, was approved for external distribution in April 2015 through Radiation Safety Information Computational Center.

*Key Words:* SILENE, uranyl nitrate, neutron activation, TLD, neutron and photon dose.

## 1. INTRODUCTION

As a part of joint effort between the US DOE Nuclear Criticality Safety Program and France, a series of neutron pulse experiment was performed in October 2010 at the Commissariat à l'Énergie Atomique et aux Énergies Alternatives (CEA) Valduc SILENE reactor in France, to provide foil and thermoluminescent dosimeter (TLD) measurement data for radiation transport code validation. During these experiments, three different single-pulse experiments were conducted including: (1) a pulse without any shielding materials around the SILENE reactor (Pulse 1), (2) a pulse with lead shielding (Pulse 2), and (3) a pulse with cadmium lined polyethylene shielding (Pulse 3). The purpose of this paper is to present COG modeling, simulation, and a complete set of COG results compared with the SILENE measurement data for the Pulse 1 experiment.

## 2. DESCRIPTION OF SILENE EXPERIMENT

SILENE is an annularly-shaped tank reactor with internal and external diameters of 7.6, and 36 cm, respectively. Fuel solution of the core consists of 93% enriched uranyl nitrate solution with a concentration of 71 grams of uranium per liter. The bottom of the fuel tank is one meter above the concrete floor. The fuel solution height varies depending on the types of experiments. In the Pulse 1 experiment, the critical fuel height was 41.871 cm with the control rod fully in. A picture of the SILENE reactor [1] without shielding material and collimators surrounding the reactor is shown in Figure 1.



**Figure 1.** SILENE Reactor and Collimators.

A cadmium control rod in the central annular region of the reactor controls the mode of operation by varying the speed with which the control rod is removed from the fuel region. Three pulse experiments were conducted in October 2010. In the Pulse 1 experiment, no shielding materials were used around the SILENE reactor. In Pulse 2, the reactor was shielded with lead. In Pulse 3, the lead shield was replaced with cadmium-lined polyethylene. The foil arrangement remained the same for all three experiments.

For Pulse 1, a single pulse was produced by removing the control rod out of the core at a rate of 2 m/sec. Approximately seven seconds later, the reactor was shut down by fully inserting the control rod into the core, and opening the valve to drain the fuel solution from the core. It took approximately thirty seconds to completely drain the fuel out of the core. Figure 2 [2] shows the fission rate versus time for the Pulse 1 experiment. A total of  $1.88 \times 10^{17}$  fissions were measured by one of the diagnostic detectors in the SILENE room.

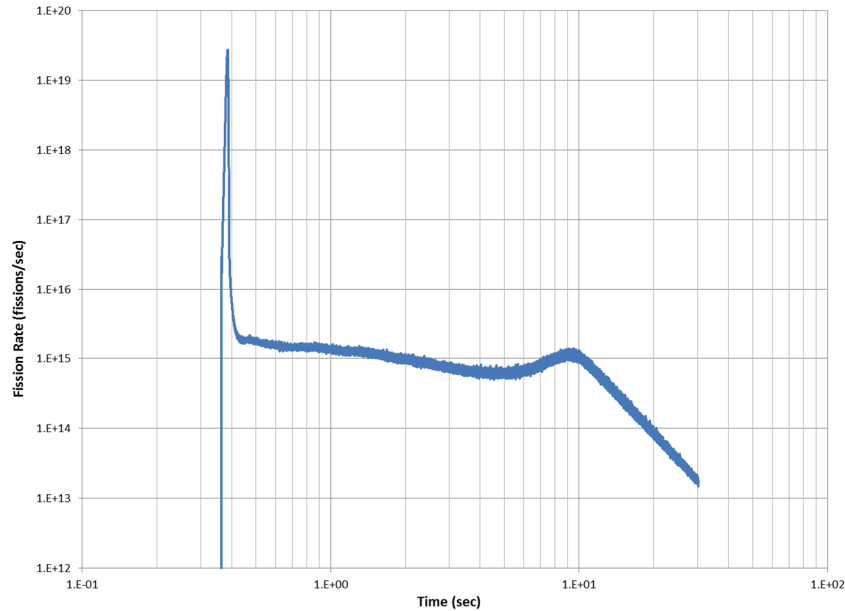


**Figure 2.** Fission Rate as a Function of Time.

During the Pulse 1 experiment, thirty-three neutron activation foils and twenty-one TLDs were utilized. The irradiated foils are small disks with a diameter of 2 cm and a thickness of less than 0.3 cm. Masses of the individual foils are less than 8 grams. The experimental configuration includes Collimator A, Collimator B, Free-field, and Scattering Box positions 1, 2, 3, and 4 (see Figure 1 for locations). The distance from the center of the SILENE reactor to Collimators A, B, and Free-field is 122 cm. The scattering box is positioned 306 cm away from the core center. A set of Co, Au, In, Fe, Mg, and/or Ni foils and TLDs were positioned in these seven different locations. To study the effect of neutron scattering, a 20-cm thick barite concrete slab was placed between the reactor and the foils and TLDs in Collimator B. The foils and TLDs in the scattering box were placed on the 20-cm thick standard and magnetite concrete slabs, with some of them shielded by the concrete slab. Two 20-cm thick magnetite concrete slabs were placed at the front and the bottom of the scattering box. Exact chemical compositions of the standard, barite, and the magnetite concrete are not known. Analysis of these concrete slabs adjusting barite, boron, and chlorine contents are described in Reference 3. Figure 3 [1] is a photograph showing a collimator foil holder with the neutron activation foils used in Collimator A, B, and Free-field. Measured activities (in Bq/g) are based on  $^{59}\text{Co}(n,\gamma)^{60}\text{Co}$ ,  $^{197}\text{Au}(n,\gamma)^{198}\text{Au}$ ,  $^{115}\text{In}(n,\gamma)^{116}\text{In}$ ,  $^{115}\text{In}(n,n'\gamma)^{115\text{m}}\text{In}$ ,  $^{56}\text{Fe}(n,p)^{56}\text{Mn}$ ,  $^{24}\text{Mg}(n,p)^{24}\text{Na}$ , and  $^{58}\text{Ni}(n,p)^{58}\text{Co}$  reactions. Note that  $^{56}\text{Fe}(n,p)$  and  $^{55}\text{Mn}(n,\gamma)$  produce the same activation product,  $^{56}\text{Mn}$ . Therefore, effect of Mn impurity in the iron foils needed to be evaluated. The trace Mn impurity in the iron foil is approximately 0.3 weight percent [4].

During the Pulse 1 experiment, four criticality accident alarm system (CAAS) detectors once used at the Rocky Flats Plant were placed in four different positions to demonstrate the functionality and survivability of the neutron detectors to the effects of an actual criticality accident. As expected, criticality alarm indicator LEDs were illuminated for the neutron pulse and functioned as intended in an actual criticality situation. The neutron detectors responded in a mixed field of neutrons and gamma rays. Three different types of TLDs were used [5] for the radiation dose measurements.

These are 1) TLDs provided by CEA Valduc consisting of an  $\text{Al}_2\text{O}_3$  powder inside an aluminum capsule, 2) HBG TLDs from ORNL, and 3) DXT TLDs from ORNL. Measurement data of all of the three different types of TLDs are reported; however, only one type (Valduc TLD) was modeled and simulated.



**Figure 3.** Collimator Foil Holder with Neutron Activation Foils.

### 3. COG MODELING AND SIMULATION

The LLNL developed COG [6] code was used for 3-D modeling the SILENE reactor and surroundings for the Pulse 1 experimental configuration. COG is a general purpose, high fidelity Monte Carlo radiation transport code that provides accurate simulation results for complex 3-D shielding, criticality, and activation problems. Point-wise continuous cross sections are used in COG and a full range of biasing options is available for speeding up solutions for deep penetration problems. These biasing options are available when a fixed source option is activated.

COG also provides two and three dimensional pictures of the model. A perspective of the three dimensional picture can be produced by enabling the user to see the inner structure hidden inside the outer surfaces. Figure 4 shows a COG generated perspective view of the SILENE reactor at the center, and the surrounding experimental configuration. Center of the perspective view and parameters of spherical coordinates were adjusted to make a picture similar to Figure 1. In COG model, each of the foils and TLDs were explicitly modeled. Rotation and translation features were utilized to accurately position the Collimator B, Free-field foils, and Scattering Box position 1, 2, 3, and 4. Note that the transient behavior of the neutron pulse (see Figure 2) was not analyzed in this study.

Flux tallies in COG with CRITICALITY option are based on a single fission. Calculated foil activity and the TLD doses are normalized to the Pulse 1 total fission of  $1.88 \times 10^{17}$  to compare with the measurement data.

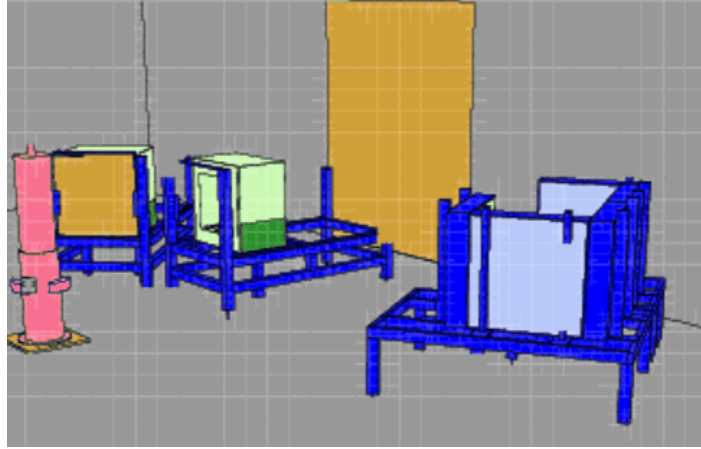


**Figure 4.** COG Perspective View of SILENE Pulse 1 Experiment Model.

Radiation dose or neutron activation analysis is normally performed in a two-step process: First, the spatial and energy dependent source distribution for a reactor is calculated. Second, a fixed source problem is solved using the generated source distribution to calculate dose or activation rate at a detector. To speed up computation time, variance reduction techniques are often applied in the fixed source (second) part of the calculation. To eliminate this biasing and/or approximations in the two-step process, a direct one-step criticality/detector calculation method was applied to all of the SILENE foil and TLD activity and dose evaluations. The only downside is that without variance reduction techniques, each calculation requires significant number computer nodes for a good statistics. COG calculates reaction rates using the CRITICALITY source and DETECTOR option in a single computer run, tracking neutrons all the way from the reactor to the detector.

The activity of the foil in Bq/g is converted using the following normalization factor,  $A$ ,

$$A = \frac{F\lambda N\sigma\Phi e^{-\lambda t}}{\rho}$$

where  $F$  is a total number of fissions,  $\lambda$  is the decay constant,  $N$  is atomic number density,  $\sigma$  is microscopic cross section,  $\Phi$  is neutron flux,  $\rho$  is foil density, and  $t$  is the time between the start of the pulse and the time when the dosimetrist reported measurement activities. Note that  $N\sigma\Phi$  is calculated by COG. Reaction rates (R-RATE option in COG) for (n, $\gamma$ ), (n,n' $\gamma$ ), and (n,p) were activated.

TLD doses were calculated using neutron/gamma ray fluence multiplied by a response function. The response function applied is the International Commission on Radiation Units and Measurements

(ICRU) air kerma flux-to-dose conversion factors [7]. A newly developed feature in COG 11.1 can track and score delayed fission gamma (DFG) rays born between two given times. This DFG option was activated to estimate additional gamma ray contribution to TLDs for the 30 second solution drainage time.

#### 4. RESULTS

COG results are compared with the measurement data in Table 1. Foil activities for Collimator A, Collimator B, Free-field, and Scattering Box positions 1, 2, 3, and 4 are presented. All of the results except for the indium foil cases are based on ENDF/B-VII.1 cross sections. In general, COG results agree reasonably well with the measurement data with the exception of a few higher predictions in the concrete-shielded foils in Collimator B. As described in Reference 4, chemical compositions of the magnetite, barite, and the standard concrete slab were determined based on incomplete composition data [1]. Actual measurements of the hydrogen, boron, chlorine, and barite contents in the concrete slabs will help for more accurate comparison of the COG results with the measurement data.

As previously published [8,9], there is an error in the measurement data of  $^{197}\text{Au}(n,\gamma)^{198}\text{Au}$  activity in Collimator A. COG calculated  $^{197}\text{Au}(n,\gamma)^{198}\text{Au}$  activity was about one-fourth of the measured value. This result is consistent with those calculated by SCALE, MCNP, and TRIPOLI [3]. The activities of indium foils were calculated using the 2002 Version of the International Reactor Dosimetry File (IRDF-2002) because of better agreement compared to ENDF/B-VII.1. Note that the calculated  $^{56}\text{Fe}(n,p)^{56}\text{Mn}$  activities in Table 1 include activities from  $^{55}\text{Mn}(n,\gamma)^{56}\text{Mn}$  reaction due to the known impurity of 0.3 wt%  $^{55}\text{Mn}$  in iron. The Mn impurity contributes more than 90% of the total activity in the iron foil.

TLD doses are also compared in Table 2. COG results agree well with the measurement data within 23% except for the Free-field and Collimator B cases. A significant discrepancy is observed for the Free-field TLD. However, the authors believe that the measured value (3.72 Gy) seems to be in error because the measured doses from the other types of TLDs (HBG and DXT) are much higher (5.02 and 5.86 Gy, respectively). Delayed fission gamma rays contributed about 10 to 15% of the total doses in the TLD doses.

**Table 1.** Comparison between Measured Foil Activities and COG Results.

Position	Measurement Data					COG		C/E	Total 1 $\sigma$ (%)
	Foil ID	Reaction	Activity (Bq/g)	2 $\sigma$ (Bq/g)	1 $\sigma$ (%)	Activity (Bq/g)	1 $\sigma$ (%)		
Collimator A	Au05-A10	$^{197}\text{Au}(n,\gamma)^{198}\text{Au}$	181200	5700	1.57%	82600	1.48%	<b>0.4559</b>	2.16%
	Ni011	$^{58}\text{Ni}(n,p)^{58}\text{Co}$	14.36	0.44	1.53%	13.69	1.42%	0.9533	2.09%
	In005	$^{115}\text{In}(n,n'\gamma)^{115\text{m}}\text{In}$	8030	250	1.56%	7640	1.05%	0.9512	1.88%
		$^{115}\text{In}(n,\gamma)^{116}\text{In}$	9.11E+06	3.5E+05	1.92%	9.76E+06	1.03%	1.0716	2.18%
	Fe021	$^{54}\text{Fe}(n,p)^{54}\text{Mn}$	0.2062	0.0082	1.99%	0.2099	1.49%	1.0179	2.48%
		$^{56}\text{Fe}(n,p)^{56}\text{Mn}$	2310	61	1.32%	2371	1.35%	1.0264	1.89%
	Mg032	$^{24}\text{Mg}(n,p)^{24}\text{Na}$	61.1	2.3	1.88%	67.7	5.84%	1.1080	6.14%
Co013	$^{59}\text{Co}(n,\gamma)^{60}\text{Co}$	66.1	1.7	1.29%	73.1	1.07%	1.1059	1.67%	
Collimator B	Au05-A10	$^{197}\text{Au}(n,\gamma)^{198}\text{Au}$	24260	750	1.5%	22428	2.74%	0.9245	3.15%
	Ni011	$^{58}\text{Ni}(n,p)^{58}\text{Co}$	2.120	0.070	1.7%	3.020	3.32%	<b>1.4245</b>	3.71%
	In005	$^{115}\text{In}(n,n'\gamma)^{115\text{m}}\text{In}$	1196	40	1.7%	1652	2.33%	<b>1.3813</b>	2.87%
		$^{115}\text{In}(n,\gamma)^{116}\text{In}$	3.00E+06	1.1E+05	1.8%	2.862E+06	2.01%	0.9539	2.72%
	Fe021	$^{54}\text{Fe}(n,p)^{54}\text{Mn}$	0.0311	0.0012	1.9%	0.0406	3.37%	<b>1.3055</b>	3.88%
		$^{56}\text{Fe}(n,p)^{56}\text{Mn}$	779	22	1.4%	714	3.03%	0.9166	3.34%
	Mg032	$^{24}\text{Mg}(n,p)^{24}\text{Na}$	10.00	0.74	3.7%	13.52	11.90%	<b>1.3520</b>	12.46%
Co013	$^{59}\text{Co}(n,\gamma)^{60}\text{Co}$	22.42	0.59	1.3%	21.46	2.01%	0.9572	2.40%	
Free-field	Au09-A10	$^{197}\text{Au}(n,\gamma)^{198}\text{Au}$	69500	2100	1.51%	76279	1.47%	1.0975	2.11%
	Ni016	$^{58}\text{Ni}(n,p)^{58}\text{Co}$	12.99	0.41	1.58%	12.75	1.48%	0.9815	2.16%
	In008	$^{115}\text{In}(n,n'\gamma)^{115\text{m}}\text{In}$	6860	220	1.60%	6768	1.07%	0.9866	1.93%
		$^{115}\text{In}(n,\gamma)^{116}\text{In}$	8.78E+06	4.3E+05	2.45%	9.35E+06	1.10%	1.0653	2.68%
	Fe028	$^{54}\text{Fe}(n,p)^{54}\text{Mn}$	0.1961	0.0081	2.07%	0.1995	1.52%	1.0173	2.56%
		$^{56}\text{Fe}(n,p)^{56}\text{Mn}$	2403	67	1.39%	2632	1.41%	1.0953	1.98%
	Mg029	$^{24}\text{Mg}(n,p)^{24}\text{Na}$	59.1	2.4	2.03%	60.98	5.74%	1.0318	6.09%
Co016	$^{59}\text{Co}(n,\gamma)^{60}\text{Co}$	66.2	1.6	1.21%	76.3	1.12%	1.1526	1.65%	

**Table 1.** Comparison between Measured Foil Activities and COG Results (Continued).

Position	Measurement Data					COG		C/E	Total 1 $\sigma$ (%)
	Foil ID	Reaction	Activity (Bq/g)	2 $\sigma$ (Bq/g)	1 $\sigma$ (%)	Activity (Bq/g)	1 $\sigma$ (%)		
Scattering Box Position 1	Au09-A10	$^{197}\text{Au}(n,\gamma)^{198}\text{Au}$	24140	730	1.5%	27654	2.47%	1.1456	2.90%
	Ni016	$^{58}\text{Ni}(n,p)^{58}\text{Co}$	0.706	0.025	1.8%	0.861	7.19%	1.2195	7.40%
	In008	$^{115}\text{In}(n,n')^{115\text{m}}\text{In}$	525	17	1.6%	532	4.36%	1.0133	4.65%
		$^{115}\text{In}(n,\gamma)^{116}\text{In}$	2.71E+06	1.0E+05	1.8%	3.15E+06	1.95%	1.1607	2.68%
	Fe028	$^{54}\text{Fe}(n,p)^{54}\text{Mn}$	0.01058	0.00078	3.7%	0.01111	7.75%	1.0501	8.58%
		$^{56}\text{Fe}(n,p)^{56}\text{Mn}$	848	22	1.3%	1011	3.74%	1.1922	3.96%
	Co016	$^{59}\text{Co}(n,\gamma)^{60}\text{Co}$	22.27	0.53	1.2%	28.45	1.96%	<b>1.2775</b>	2.29%
Scattering Box Position 2	Au10-A10	$^{197}\text{Au}(n,\gamma)^{198}\text{Au}$	25390	830	1.6%	32330	2.29%	<b>1.2733</b>	2.81%
	Ni015	$^{58}\text{Ni}(n,p)^{58}\text{Co}$	0.290	0.012	2.1%	0.37	10.43%	<b>1.2759</b>	10.63%
	Co022	$^{59}\text{Co}(n,\gamma)^{60}\text{Co}$	25.59	0.56	1.1%	32.74	1.83%	<b>1.2794</b>	2.13%
Scattering Box Position 3	Au10-A10	$^{197}\text{Au}(n,\gamma)^{198}\text{Au}$	44600	1400	1.57%	51781	1.75%	1.1610	2.35%
	Ni015	$^{58}\text{Ni}(n,p)^{58}\text{Co}$	3.24	0.11	1.70%	3.29	2.84%	1.0154	3.31%
	Co022	$^{59}\text{Co}(n,\gamma)^{60}\text{Co}$	44.04	0.99	1.12%	53.17	1.41%	1.2073	1.80%
Scattering Box Position 4	Au03-A10	$^{197}\text{Au}(n,\gamma)^{198}\text{Au}$	38700	1200	1.55%	46412	1.88%	1.1993	2.44%
	Ni024	$^{58}\text{Ni}(n,p)^{58}\text{Co}$	3.33	0.11	1.65%	3.41	4.27%	1.0240	4.58%
	Co009	$^{59}\text{Co}(n,\gamma)^{60}\text{Co}$	39.93	0.87	1.09%	46.81	1.53%	1.1723	1.88%

**Table 2.** COG Calculated TLD Doses Compared with the Measurement Data.

Position	Measured Data (Gy)	1 $\sigma$ (%)	Delayed Fission Gamma	COG						C/E	Total 1 $\sigma$ (%)
				Neutron Dose (Gy)	1 $\sigma$ (%)	Gamma Ray Dose (Gy)	1 $\sigma$ (%)	Total (Gy)	1 $\sigma$ (%)		
Collimator A	6.61	2.20	w/o DFG	1.22	1.41	4.59	1.70	5.81	2.21	0.88	3.12
			w/ DFG	1.22	1.42	5.18	1.54	6.40	2.09	0.97	3.04
Collimator B	0.82	1.70	w/o DFG	0.26	2.97	0.74	4.30	1.00	5.23	1.22	5.50
			w/ DFG	0.29	2.90	0.81	4.17	1.10	5.08	<b>1.34</b>	5.36
Free-field	3.72	2.50	w/o DFG	1.07	1.53	3.87	1.52	4.94	2.16	<b>1.33</b>	3.30
			w/ DFG	1.12	1.87	4.64	1.66	5.76	2.50	<b>1.55</b>	3.54
Scattering Box Position 1	0.58	2.00	w/o DFG	0.24	3.18	0.40	5.96	0.64	6.76	1.10	7.05
			w/ DFG	0.24	3.12	0.46	5.65	0.70	6.45	1.21	6.76
Scattering Box Position 2	0.44	1.60	w/o DFG	0.26	3.03	0.28	6.78	0.54	7.43	1.23	7.59
			w/ DFG	0.24	3.14	0.30	6.25	0.54	6.99	1.23	7.16
Scattering Box Position 3	1.76	1.20	w/o DFG	0.53	2.19	1.08	3.31	1.61	3.97	0.91	4.15
			w/ DFG	0.52	2.19	1.37	3.05	1.89	3.75	1.07	3.94
Scattering Box Position 4	1.87	2.95	w/o DFG	0.48	2.20	1.14	3.26	1.62	3.93	0.87	4.92
			w/ DFG	0.53	2.22	1.32	3.00	1.85	3.73	0.99	4.76

## 5. CONCLUSIONS

This work demonstrated that the one-step COG criticality/detector calculations are valid for foil activation and TLD dose evaluations. Unlike the two-step criticality/fixed source calculations, there are no biasing/approximation in neutron source generation. Inclusion of newly developed delayed fission gamma feature contributed about 10 to 15% of the total gamma ray doses in TLDs. To reduce calculation uncertainties for small foil tally volumes, additional large scale runs on massive parallel supercomputers are needed. To this end, a new one-step hybrid criticality/shielding-detector method was developed, and a message passing interface (MPI) feature is being added to allow COG to run in parallel on a multiprocessor machine. A Criticality Detector Variance Reduction (CritDetVR) mode allows users to apply variance reduction methods in the one-step criticality/shielding calculation. COG interleaves criticality batches with shielding cycles in such a way that each shielding cycle transports the source neutrons generated by the preceding criticality batch. Each shielding cycle can employ any of the variance reduction methods to enhance scoring statistics at the detectors. The latest version, COG11.1 was approved for external distribution in April 2015 through Radiation Safety Information Computational Center.

## ACKNOWLEDGMENTS

The authors would like to thank Thomas Miller at ORNL, and the CEA Staff for providing design and experimental information on the SILENE first pulse experiment. This work was performed under the auspices of the U.S. Department of Energy by Lawrence Livermore National Laboratory under Contract DE-AC52-07NA27344 and was funded by the U.S. Department of Energy Nuclear Criticality Safety Program.

## REFERENCES

- [1] J. Piot, “2010 CAAS Test on the SILENE Reactor, Data for CAAS Experiment Modeling,” CEA/VA/DRMN/SRNC DO 428, Commissariat à l’Énergie Atomique et aux Énergies Alternatives (2011)
- [2] T. M. Miller, et. al., Neutron Activation and Thermoluminescent Detector Responses to a Bare Pulse of the CEA Valduc SILENE Criticality Assembly, ALARM-TRANS-AIR-SHIELD-001, International Handbook of Evaluated Criticality Safety benchmark Experiments, NEA/NSC/DOC(95)03, OECD/NEA (September 2015 Edition)
- [3] T. M. Millers, et. al., “Evaluation of the Concrete Shield Compositions from the 2010 Criticality Accident Alarm System Benchmark Experiments at the CEA Valduc SILENE Facility,” Proc. Int. Conf. *International Conference on Nuclear Criticality Safety*, Charlotte, North Carolina, September 13 – 17, pp. 1647-1658, on CD-ROM (2015)
- [4] RAPPORT D’ESSAIS – DOSSIER D’EXPERIENCE N°2011/014.a, Center de Valduc, CEA (2011)
- [5] T. M. Miller, et. al., “2010 Criticality Alarm System Benchmark Experiments at the CEA VALDUC SILENE Reactor,” Proc. Int. Conf. *2011 International Conference on Nuclear Criticality*, Track 4.26, September 19-22, Edinburgh, UK (2011)
- [6] *COG: A Multiparticle Monte Carlo Code Transport Code, Version 11.1*, CCC-829, Released by Radiation Safety Information Computational Center (2015)
- [7] ICRU-57, “Conversion Coefficients for Use in Radiological Protection Against External Radiation,” International Commission on Radiation Units and Measurements, Bethesda, MD (1998)
- [8] T. M. Millers, et. al., “Analysis of Measured Data from Experiments 2 and 3 of the 2010 Criticality Accident Alarm System Benchmark at the CEA Valduc SILENE Facility,” Proc. Conf. *ANS 2013 Nuclear Criticality Safety Division Topical Meeting*, Wilmington, North Carolina, September 29 – October 3, on CD-ROM (2013)
- [9] S. Kim, D. Heinrichs, R. Buck, E. Lent, and C. Lee, “COG Preliminary Results for a SILENE Criticality Excursion Benchmark Experiment,” *Transactions of American Nuclear Society*, Vol. 108, pp. 463-465 (2013)